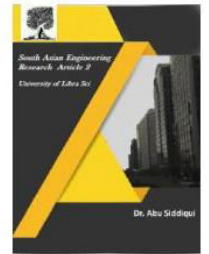




2581-4575



## A Multilevel Inverter Based on Switched Capacitor for High-Frequency Power Distribution System

V Vinay Kumar<sup>1</sup>, Bhav Singh<sup>2</sup>

<sup>1</sup> Assistant professor, Dept. of EEE, RGUKT Basar, Telangana-504107, India

<sup>2</sup> Assistant professor, Dept. of EEE, RGUKT Basar, Telangana-504107, India

*Abstract*—The increase of transmission frequency reveals more merits than low- or medium-frequency distribution among different kinds of power applications. High-frequency inverter serves as source side in high-frequency ac (HFAC) power distribution system (PDS). However, it is complicated to obtain a high-frequency inverter with both simple circuit topology and straightforward modulation strategy. A novel switched-capacitor-based cascaded multilevel inverter is proposed in this paper, which is constructed by a switched-capacitor frontend and H-Bridge backend. Through the conversion of series and parallel connections, the switched-capacitor frontend increases the number of voltage levels. The output harmonics and the component counter can be significantly reduced by the increasing number of voltage levels. A symmetrical triangular waveform modulation is proposed with a simple analog implementation and low modulation frequency comparing with traditional multicarrier modulation. The circuit topology, symmetrical modulation, operation cycles, Fourier analysis, parameter determination, and topology enhancement are examined.

### I INTRODUCTION

A traditional HFAC PDS is made up of a high-frequency (HF) inverter, an HF transmission track, and numerous voltage-regulation modules (VRM). HF inverter accomplishes the power conversion to accommodate the requirement of point of load (POL). In order to increase the power capacity, the most popular method is to connect the inverter output in series or in parallel. However, it is impractical for HF inverter, because it is complicated to simultaneously synchronize both amplitude and phase with HF dynamics. Multilevel inverter is an effective solution to increase power capacity without synchronization consideration, so the higher power capacity is easy to be achieved by multilevel inverter with lower switch stress. Nonpolluted sinusoidal waveform with the lower total harmonic distortion (THD) is critically caused by long track distribution in HFAC PDS. The higher number of voltage levels can effectively decrease total harmonics content of stair-case output, thus significantly simplifying the filter design [7]. HF power distribution is applicable for small-scale and internal closed electrical network in electric vehicle (EV) due to moderate size of distribution network and effective weight reduction [8]. The consideration of operation frequency has to make compromise between the ac inductance and resistance [9], so multilevel inverter with the output frequency of about 20 kHz is a feasible trial to serve as power source for HF EV application.

The traditional topologies of multilevel inverter mainly are diode-clamped and capacitor-clamped type [10], [11]. The former uses diodes to clamp the voltage level, and the latter

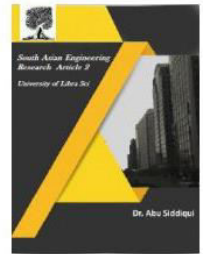


2581-4575

# International Journal For Recent Developments in Science & Technology



A Peer Reviewed Research Journal



uses additional capacitors to clamp the voltage. The higher number of voltage levels can then be obtained; however, the circuit becomes extremely complex in these two topologies. Another kind of multilevel inverter is cascaded H-Bridge constructed by the series connection of H-Bridges [12], [13]. The basic circuit is similar to the classical H-bridge DC-DC converter [14]. The cascaded structure increases the system reliability because of the same circuit cell, control structure and modulation. However, the disadvantages confronted by cascaded structure are more switches and a number of inputs. In order to increase two voltage levels in staircase output, an H-Bridge constructed by four power switches and an individual input are needed. Theoretically, cascaded H-Bridge can obtain staircase output with any number of voltage levels, but it is inappropriate to the applications of cost saving and input limitation.

Since the carrier frequency determines the switching frequency, a high switching loss is inevitable for the sake of high-frequency output. A boost multilevel inverter based in partial charging of SC can increase the number of voltage levels theoretically. However, the control strategy is complicated to implement partial charging [20]. Therefore, it is a challenging task to present an SC-based multi-level inverter with high-frequency output, low-output harmonics, and high conversion efficiency [21].

Based on the study situation aforementioned, a novel multi-level inverter and simple modulation strategy are presented to serve as HF power source. The rest of this paper is organized as follows. The discussions of nine-level inverter are presented in Section II, including circuit topology, modulation strategy, operation cycle, and Fourier analysis. The parameter determination and loss analysis are discussed in Section III. The further enhancement of 13-level inverter is studied in Section IV. The performance evaluation accomplished by simulation and experiment is described in Section V followed by concluding remarks.

## SC-BASED CASCADED INVERTER WITH NINE-LEVEL OUTPUT

The proposed circuit is made up of the SC frontend and cascaded H-Bridge backend. If the numbers of voltage levels obtained by SC frontend and cascaded H-Bridge backend are  $N_1$  and  $N_2$ , respectively, the number of voltage levels is  $2 \times N_1 \times N_2 + 1$  in the entire operation cycle.

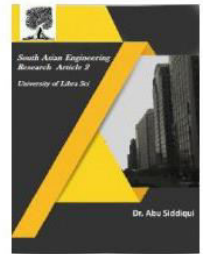
### A. Circuit Topology

Fig. 1 shows the circuit topology of nine-level inverter ( $N_1 = 2, N_2 = 2$ ), where  $S_1, S_2, S_1, S_2$  as the switching devices of SC circuits (SC1 and SC2) are used to convert the series or parallel connection of  $C_1$  and  $C_2$ .  $S_{1a}, S_{1b}, S_{1c}, S_{1d}, S_{2a}, S_{2b}, S_{2c}, S_{2d}$  are the switching devices of cascaded H-Bridge.  $V_{d c1}$  and  $V_{d c2}$  are input voltage.  $D_1$  and  $D_2$  are diodes to restrict the current direction.  $i_{o u t}$  and  $v_o$  are the output current and the output voltage, respectively.

It is worth noting that the backend circuit of the proposed inverter is cascaded H-Bridges in series connection. It is significant for H-Bridge to ensure the circuit conducting regardless of



2581-4575



the directions of output voltage and current. In other words, H-Bridge has four conducting modes in the conditions of inductive and resistive load, i.e., forward conducting, reverse conducting, forward freewheeling, and reverse freewheeling.

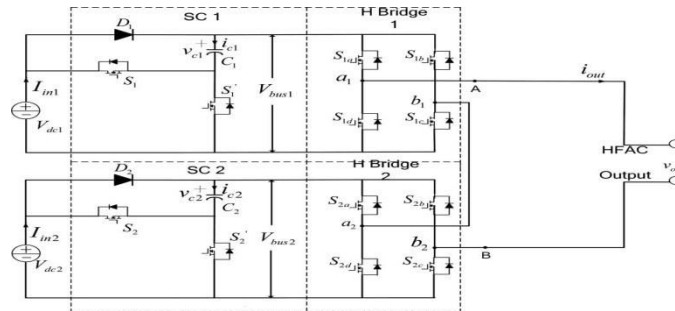


Fig Circuit topology of cascaded nine-level inverter ( $N_1 = 2, N_2 = 2$ ).

### B. Symmetrical Modulation

There are many modulation methods to regulate the mul-tilevel inverter, the popular modulations are the space vector modulation [22], the multicarrier PWM [23], and the selective harmonic elimination [24], [25], subharmonic pulsewidth modulation [26], etc. However, most of them greatly increase the carrier frequency that is dozens times the frequency of refer-ence or output. A symmetrical phase-shift modulation (PSM) is introduced into the proposed multilevel inverter. The sym-metrical PSM ensures the output voltage of full bridge is sym-metrical to the carrier, so voltage levels can be superimposed symmetrically and carrier frequency is twice as that of the out-put frequency [27]. The structure of symmetrical PSM is shown in Fig. 2(a), and the operational waveform of symmetrical PSM is shown in Fig. 2(b).

The logic operations of gate signals are

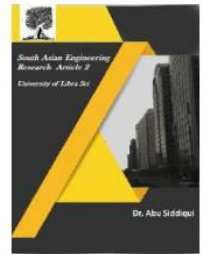
$$\begin{aligned}
 \text{gate} &= - \\
 1 &= X \text{ OR} \{Q(RS), Q(D)\} \\
 \text{gate} &= X \text{ OR} \{Q(RS), Q(D)\} & (1) \\
 2 &= X \text{ OR} \{Q(RS), Q(D)\} & ) \\
 \text{gate} &= X \text{ OR} \{AN D\{Q(RS), N OT (P W M )\}, \\
 3 &Q(D)\} \\
 &- \\
 \text{gate} &= X \text{ OR} \{AN D\{Q(RS), N OT (P W M )\}, \\
 4 &Q(D)\}.
 \end{aligned}$$

### C. Operation Cycles

Fig. 3 demonstrates the ideal waveforms of proposed inverter.  $V_c$  is the triangular carrier, and  $V_{p,p}$  is the peak value of  $V_c$ . The modulation signals of triangular carrier are  $V_{m1c}, V_{m1b}, V_{m2c}$  and  $V_{m2b}$ .  $V_{m1b}$  and  $V_{m2b}$  are used to control phase-shift angles of H-Bridge 1 and H-Bridge 2, respectively, and  $\delta_i$  is the duration of voltage levels controlled by them.  $V_{m1c}$  and  $V_{m2c}$  are used to control the alternative operations of SC1 and SC2, respectively, and  $\alpha_i$  is the duration of



2581-4575



voltage levels controlled by them. Thus, the drive signals of H-Bridge switches ( $S_{1a}$ ,  $S_{1b}$ ,  $S_{1c}$ ,  $S_{1d}$ ,  $S_{2a}$ ,  $S_{2b}$ ,  $S_{2c}$ ,  $S_{2d}$ ) are phase-shifted pulse signals, while the drive signals of SC switches ( $S_1$ ,  $S_2$ ,  $S_1$ ,  $S_2$ ) are complementary pulse signals. Two operational modes are presented as shown in Fig. 3(a) and (b). Mode 1 is similar to mode 2 apart from the different positions of modulation signals ( $V_{m1c}$ ,  $V_{m1b}$ ,  $V_{m2c}$ ,  $V_{m2b}$ ). Consequently, the durations of each voltage level are controlled by modulation signals in both mode 1 and mode 2.

Active circuits of the operational mode 1 are demonstrated in Fig. 4.  $R_e$  is the equivalent load. When  $t$  satisfies  $t_0 \leq t$

$< t_1$  in Fig. 3(a), the switches  $S_{1a}$ ,  $S_{1b}$ ,  $S_{2a}$ ,  $S_{2b}$  are driven by the gate-source voltage, respectively. H-Bridges 1 and 2 are in freewheeling state, and output voltage equals 0. Because  $S_1$  and  $S_2$  are on, the capacitors  $C_1$  and  $C_2$  are charged to  $V_{in}$

( $V_{dc1} = V_{dc2} = V_{in}$ ). The voltages on Bus 1 and Bus 2 are  $V_{in}$  as well.

When  $t$  satisfies  $t_1 \leq t < t_2$  in Fig. 3(a), the switches  $S_{1a}$ ,  $S_{1b}$ ,  $S_{2a}$ ,  $S_{2c}$  are driven by the gate-source voltage, respectively. H-Bridge 1 is in freewheeling state, and H-Bridge 2 is in positive conducting state. Output voltage equals  $V_{in}$ . Because  $S_1$  and  $S_2$  are on, the capacitors  $C_1$  and  $C_2$  keep charged to  $V_{in}$  ( $V_{dc1} = V_{dc2} = V_{in}$ ). The voltages on Bus 1 and Bus 2 are  $V_{in}$  as well. The current flow of this time interval is shown in Fig. 4(b).

When  $t$  satisfies  $t_2 \leq t < t_3$  in Fig. 3(a), the switches  $S_{1a}$ ,  $S_{1c}$ ,  $S_{2a}$ ,  $S_{2c}$  are driven by the gate-source voltage, respectively. H-Bridges 1 and 2 are in positive conducting state. Output voltage equals  $2V_{in}$ . Because  $S_1$  and  $S_2$  are on, the capacitors  $C_1$  and  $C_2$  keep charged to  $V_{in}$  ( $V_{dc1} = V_{dc2} = V_{in}$ ). The voltages on Bus 1 and Bus 2 are  $V_{in}$  as well. The current flow of this time interval is shown in Fig. 4(c).

When  $t$  satisfies  $t_3 \leq t < t_4$  in Fig. 3(a), the switches  $S_{1a}$ ,  $S_{1c}$ ,  $S_{2a}$ ,  $S_{2c}$  are driven by the gate-source voltage, respectively. H-Bridges 1 and 2 are in positive conducting state. Output voltage equals  $3V_{in}$ . Because  $S_1$  and  $S_2$  are on, the capacitor  $C_1$  keeps charged to  $V_{in}$  ( $V_{dc1} = V_{dc2} = V_{in}$ ), and the capacitor  $C_2$  is discharged. The voltages on Bus 1 and Bus 2 are  $V_{in}$  and  $2V_{in}$ , respectively. The current flow of this time interval is shown in Fig. 4(d).

### III. DETERMINATION OF CAPACITANCE

As shown in Fig. 4, the capacitors are charged when they are in parallel with power source, and the capacitors are discharged when they are in series with power source. The switch  $S_i$  and  $S_i$  are driven alternatively during the half of output cycle. Therefore, the driven frequency of  $S_i$  and  $S_i$  is twice the frequency of output voltage, as well as the driven frequency of  $S_{ia} - S_{id}$  is the same as the frequency of output voltage

The capacitance of  $C_i$  is determined by the voltage ripple of  $C_i$  that denotes the voltage fluctuation of multilevel output. The larger capacitance has the fewer ripple voltage. The voltage fluctuation over a narrow scope has a smaller power losses and higher capacitor

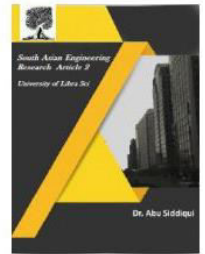


2581-4575

# International Journal For Recent Developments in Science & Technology



A Peer Reviewed Research Journal



efficiency. The appropriated method of capac- itance calculation is that the maximum voltage ripple is 10% of the maximum capacitor voltage

It can be seen from the equations that the operational mode needs larger  $C_2$  than that in operational mode 1. When the load is resistive, the phase of load current is agreed with the load voltage. The maximum discharging amount of capacitor is obtained in resistive load, because the peak load current is the midpoint of integration period. In other words, if the capacitance of  $C_i$  is derived in pure resistive load, it also maintains the less voltage ripples in inductive load. The peak current of the capacitor  $C_i$  is derived by Where  $V_{Ci}$  is the voltage on the capacitors  $C_i$ ,  $V_{dF}$  is the forward voltage drop of diode,  $r_c$  is the equivalent series resistance (ESR) of the capacitors,  $r_{on}$  is the internal on-state resistance of the switching device, and  $r_d$  is the internal on-state resistance of the diode. Because of a small voltage difference of  $V_{in}$  and  $V_{Ci}$ , the peak current  $I_{ci}$  is fewer for the larger  $C_i$ . Thus, the larger capacitor is needed to cut down undesirable peak current and prolong the capacitor lifetime. The analysis of switching loss is similar to the traditional cascaded H-bridge, while the capacitor losses consisting of ripple loss  $P_{rip}$  and conduction loss  $P_{cond}$  are newly introduced by the proposed inverter. When the capacitor  $C_i$  is connected from series to parallel, the ripple is derived by the difference between the input voltage  $V_{in}$  and the capacitor voltage  $V_{ci}$ . The voltage ripple of  $C_i$  is where  $V_{Ci}$  is the voltage on the capacitors  $C_i$ ,  $V_{dF}$  is the forward voltage drop of diode,  $r_c$  is the equivalent series resistance (ESR) of the capacitors,  $r_{on}$  is the internal on-state resistance of the switching device, and  $r_d$  is the internal on-state resistance of the diode. Because of a small voltage difference of  $V_{in}$  and  $V_{Ci}$ , the peak current  $I_{ci}$  is fewer for the larger  $C_i$ . Thus, the larger capacitor is needed to cut down undesirable peak current and prolong the capacitor lifetime.

The analysis of switching loss is similar to the traditional cas- caded H-bridge, while the capacitor losses consisting of ripple loss  $P_{rip}$  and conduction loss  $P_{cond}$  are newly introduced by the proposed inverter. When the capacitor  $C_i$  is connected from series to parallel, the ripple is derived by the difference between the input voltage  $V_{in}$  and the capacitor voltage  $V_{ci}$ . The voltage ripple of  $C_i$  is fine.

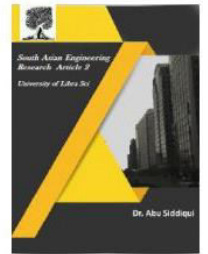
## FURTHER ENHANCEMENTS

The number of voltage levels can be further increased via two approaches. One is to increase the level number generated by SC circuit; the other one is to increase level number generated by cascaded H-Bridge. Thirteen-level inverters, as shown in Fig. 9, explain these two methods.

A  $3 \times 2$  structure, as shown in Fig. 9(a), is derived by the enhancement of SC circuit, which needs 6 diodes, 4 capacitors, 14 switches, and 2 dc inputs.  $2 \times 3$  structure as shown in Fig. 9(b) is derived by the enhancement of H-Bridge circuit, which needs 3 diodes, 3 capacitors, 18 switches, and 3 dc inputs. It can be found that  $3 \times 2$  structure requires more diodes and capacitors than  $2 \times 3$  structure. However, the number of power switches in  $3 \times 2$  structure is less than that in  $2 \times 3$  structure. Because the traditional cascaded H-bridge



2581-4575



needs 24 switches and 6 inputs to produce 13 voltage levels, the numbers of power switches and inputs are greatly decreased by proposed inverter. In order to accomplish the staircase output with  $4n + 1$  voltage levels, the component counts are compared in Table II.

TABLE II  
COMPONENTS COMPARISON OF PROPOSED INVERTER AND  
CASCADED H-BRIDGE

Inverter type	Proposed inverter enhanced by SC $n \times 2$ topology	Proposed inverter enhanced by H-Bridge $2 \times n$ topology	Cascaded H-Bridge
Switching device	$2n+8$	$6n$	$8n$
Capacitor	$2n-2$	$n$	0
Diode	$4n-6$	$n$	0
DC bus	2	$n$	$2n$
Power losses	$(2n-2)loss_{cap}+(4n-6)loss_{diode}+(2n+8)loss_{switch}$	$nloss_{cap}+nloss_{diode}+6nloss_{switch}$	$8nloss_{switch}$

An  $n \times 2$  topology needs  $2n - 2$  capacitors,  $2n + 8$  switches, and 2 dc inputs;  $2 \times n$  topology needs  $n$  capacitors,  $6n$  switches, and  $n$  dc inputs. The traditional cascaded H-Bridge needs  $8n$  switches and  $2n$  dc inputs. With the same number of voltage levels, the proposed inverter needs less switching devices and inputs than the traditional cascaded H-Bridge. Considering the power losses, the traditional cascaded H-bridge has the higher switching losses caused by more switch devices. However, the proposed inverter newly introduces the capacitor loss that has already been examined in last section. Moreover, a flexible circuit structure becomes possible. It is feasible for the proposed multilevel inverter to select suitable enhancement that can accommodate the requirements from different applications. For example,  $2 \times n$  topology can be used for the power application sourced by multiple solar panels or batteries, and  $n \times 2$  topology can be used for the power application sourced by dual power sources.

## CONCLUSION

In this paper, a novel SC-based cascaded multilevel inverter was proposed. Both 9-level and 13-level circuit topology are examined in depth. Compared with conventional cascaded multilevel inverter, the proposed inverter can greatly decrease the number of switching devices. A single carrier modulation named by symmetrical PSM, was presented with the low switching frequency and simple implementation. The accordant results of simulation and experiment further confirm the feasibility of proposed circuit and modulation method.

Comparing with traditional cascade H-bridge, the number of voltage levels can be further increased by SC frontend. For instance, the number of voltage levels increases twice in half cycle of 9-level circuit, and the number of voltage levels increases three times in half cycle of 13-level circuit. With the exponential increase in the number of voltage levels, the har-

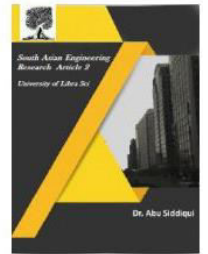


2581-4575

# International Journal For Recent Developments in Science & Technology



A Peer Reviewed Research Journal



monics are significantly cut down in staircase output, which is particularly remarkable due to simple and flexible circuit topol-ogy. Meanwhile, the magnitude control can be accomplished by pulsewidth regulation of voltage level, so the proposed mul-tilevel inverter can serve as HF power source with controlled magnitude and fewer harmonics. This paper mainly analyzes nine-level and 13-level inverters. The method of analysis and design is also applicable to other members of the proposed in-verter.

## REFERENCES

- [1] P. Jain and H. Pinheiro, "Hybrid high frequency AC power distribution ar-chitecture for telecommunication systems," *IEEE Trans. Aerospace Elec-tron. Syst.*, vol. 35, no. 1, pp. 138–147, Jan. 1999.
- [2] J. Drobniak, "High frequency alternating current power distribution," in *Proc. 16th Int.Telecommun. Energy Conf., (INTELEC '94)*, Oct. 30–Nov.3, pp. 292–296.
- [3] B. K. Bose, M.-H. Kin, and M. D. Kankam, "High frequency AC vs. DC distribution system for next generation hybrid electric vehicle," in *Proc.IEEE Int. Conf. Ind. Electron., Control, Instrum. (IECON)*, Aug. 5–10,1996, vol. 2, pp. 706–712.
- [4] S. Chakraborty and M. G. Simoes, "Experimental evaluation of active filtering in a single-phase high-frequency AC microgrid," *IEEE Trans.Energy Convers.*, vol. 24, no. 3, pp. 673–682, Sep. 2009.
- [5] R. Strzelecki and G. Benysek, *Power Electronics in Smart ElectricalEnergy Networks*. London, U.K.: Springer-Verlag, 2008.
- [6] Z. Ye, P. K. Jain, and P. C. Sen, "A two-stage resonant inverter with control of the phase angle and magnitude of the output voltage," *IEEE Trans. Ind.Electron.*, vol. 54, no. 5, pp. 2797–2812, Oct. 2007.
- [7] L. M. Tolbert, F. Z. Peng, and T. G. Habetler, "Multilevel PWM methods at low modulation indices," *IEEE Trans. Power Electron.*, vol. 15, no. 4, pp. 719–725, Jul. 2000.